STUDIECENTRUM VOOR KERNENERGIE

CENTRE D'ETUDE DE L'ENERGIE NUCLEAIRE

FAST NEUTRON IRRADIATION INDUCED SWELLING OF METALS AND ALLOYS

L. Stals

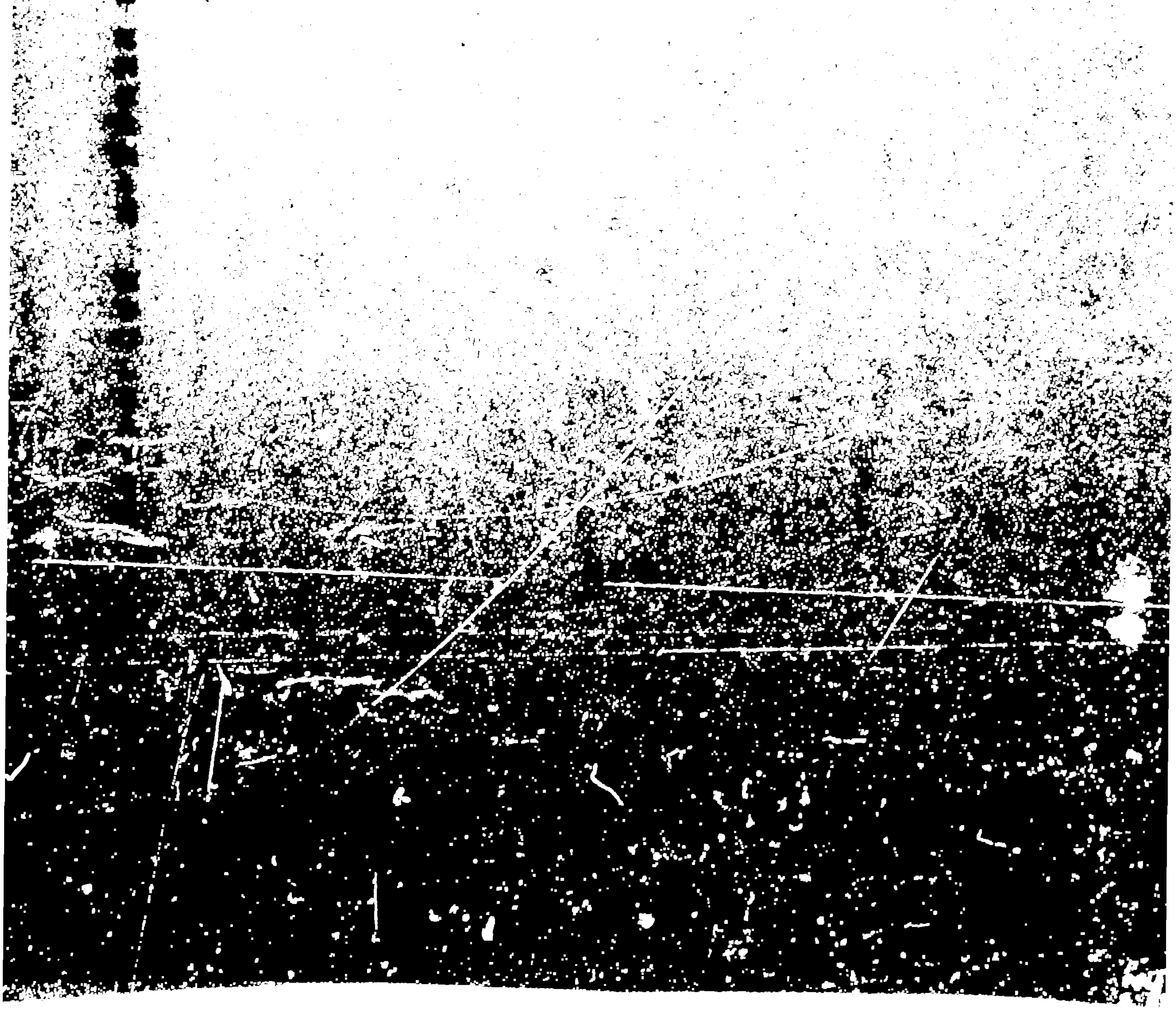

FAST NEUTRON IRRADIATION INDUCED SWELLING OF METALS AND ALLOYS

L. Stals

BLG 457

This work was carried out as part of the workprogramme of the Gas Breeder Reactor Association Study Group in Brussels, Belgium

L. STALS
BLG 457 (Dec. 1970)

FAST NEUTRON IRRADIATION INDUCED SWELLING OF METALS AND ALLOYS

Summary. - This paper deals with a literature study of the experimental data on the swelling behaviour of metals and alloys as observed after fast neutron irradiations. The experimental data show that pure metals and alloys behave quite similarly as far as swelling is concerned. The threshold dose for swelling is for most metals a few orders of magnitude lower than for alloys. The temperature dependence of the swelling, however, is comparable. Theory predicts that in austenitic steel AISI type 304 and 316 swelling should saturate at $\frac{\Delta v}{v} \simeq 12$ %. There is also some experimental evidence for saturation below $\frac{\Delta v}{v} \simeq 20$ %.

L. STALS
BLG 457 (Dec. 1970)

FAST NEUTRON IRRADIATION INDUCED SWELLING OF METALS AND ALLOYS

Samenvatting. - Dit rapport behandelt een literatuurstudie van de experimentele gegevens over het zwelling-gedrag van metalen en legeringen bij bestraling met snelle neutronen. De experimentele gegevens tonen aan dat zwelling van zuivere metalen en legeringen gelijkaardig is met dit verschil echter dat de drempeldosis voor zwelling voor de meeste metalen enkele grootte-orden lager is dan voor legeringen. De temperatuurafhankelijkheid van de zwelling is echter vergelijkbaar. De teorie voorspelt dat in austenistisch staal AISI types 304 en 316 zwelling zou verzadigen bij $\frac{\Delta v}{v} \simeq 12$ %. Er bestaan eveneens experimentele aanwijzingen voor verzadiging onder $\frac{\Delta v}{v} \simeq 20$ %.

L. STALS
BLG 457 (Dec. 1970)

FAST NEUTRON IRRADIATION INDUCED SWELLING OF METALS AND ALLOYS

Résumé. - Le présent rapport porte sur une étude de la littérature relative aux données expérimentales concernant le gonflement de métaux et d'alliages sous irradiation aux neutrons rapides. Les données expérimentales montrent que le comportement sous gonflement des métaux purs et des alliages est pratiquement identique. La dose seuil pour le gonflement est pour la plupart des métaux quelques ordres de grandeur plus basse que celle pour des alliages. Par contre, la dépendance de température du gonflement est comparable. La théorie prévoit que le gonflement serait saturé à $\frac{\Delta v}{v} \simeq 12$ % dans l'acier austénitique AISI types 304 et 316. Il y a également des indications expérimentales pour la saturation en-dessous de $\frac{\Delta v}{v} \simeq 20$ %.

FAST NEUTRON IRRADIATION INDUCED SWELLING OF METALS AND ALLOYS

L. STALS

1. Introduction

In designing and developing an economical fast breeder reactor, the engineer is confronted with the problem of the dimensional stability of the reactor structural components (core components, fuel-element cladding...). Normal working conditions of a future fast reactor will be rather severe : the reactor structural components will be subjected to neutron fluxes in excess of 10^{15} n cm^{-2} s^{-1} (E > 0.1 MeV) up to fluences in excess of 10^{23} n cm^{-2} (corresponding to a safe continuous operation period of about 3 years) and at temperatures between 350°C and 700°C (to obtain an economical thermodynamical output).

Among the various candidate alloys the austenitic stainless steels seem to be promising materials in various aspects. However, as it is the case for most metals and alloys, austenitic steel is dimensionally unstable under the above-mentioned fast reactor conditions. The main sources of this instability are creep and swelling. Although a large number of experimental data have become available during the last few years, the processes resulting in fast neutron irradiation induced swelling and creep are still poorly understood. The swelling of irradiated metals and alloys is the result of void formation due to the high supersaturation of vacancies formed during neutron bombardment. Creep under irradiation may possibly be caused both by enhanced climb of dislocations due to the point defect supersaturation and by the change of microstructure due to dislocation loops and voids.

The present report deals with a survey on the swelling of metals and alloys as observed after fast neutron irradiation. Two techniques are currently used for studying the swelling phenomenon : transmission electron microscopy (T.E.M.) allows observation and study of void sizes, void crystallography, void distribution and void densities whereas immersion density measurements are used to investigate macroscopic swelling. From the void sizes and void densities as derived from T.E.M. observations one is able to compute total volumes, which can be compared to macroscopic volume increases.

Cawthorne and Fulton (1, 2) were the first investigators to report on the observation of fast neutron induced voids in austenitic stainless steel AISI type 316. They made T.E.M. observations on samples irradiated in the Dounreay Fast Reactor in the temperature range 400-610°C up to fast fluences in excess of 10^{22} n cm^{-2}. After irradiation below 350°C, they observed the presence of the usual black dots, which grew into resolvable loops during annealing. After irradiation above 350°C, however, a new type of irradiation-produced extended defect became visible, which is now widely called "void"*. The voids appeared in the electron microscope as spherical or polyhedral cavities ranging in size from the smallest observable to 1 500 Å. Calculation of the concentration of neutronic gas showed that this concentration was a few orders of magnitude too low to fill the voids up to the equilibrium

---

*Voids have been observed earlier in quenched metals (see e.g. E. Ruedl, P. Delavignette and S. Amelinckx, J. Nucl. 6, 46, 1962) and in diffusion experiments in relation to the Kirkendall effect (see e.g. F. Seitz, Acta Met. 1, 355, 1953).

Laplace pressure, as it is the case for gas bubbles which had been observed before in irradiated stainless steel. Therefore, Cawthorne and Fulton concluded that the observed voids are relatively empty cavities produced by the condensation of vacancies on gaseous nuclei resulting from nuclear reactions. This conclusion was supported by annealing experiments. After annealing at 700°C for 1 hour the voids were relatively unchanged, whereas annealing at 900°C for 1 hour removed the voids completely leaving a residue whose volume was roughly equal to the neutronic gas content at a pressure equal to the equilibrium Laplace pressure.
It has also been observed that the total void volume and, as a consequence, the macroscopic swelling, depend on temperature (see table I).

TABLE I

Swelling data for AISI 316 stainless steel (1, 2)

Total neutron dose (n cm^{-2})	Estimated irradiation temperature (°C)	Average void diameter (Å)	Total void volume (%)	Immersion density measurements $\frac{\Delta V}{V}$ (%)
5.2×10^{22}	450	135	0.8	-
7.8×10^{22}	500	1 100	7	7
4.5×10^{22}	510	252	1.5	-
3.2×10^{22}	560	258	0.2	-

After these observations by Cawthorne and Fulton, it soon became clear that the swelling phenomenon would influence the dimensional stability of fast reactor components. As a consequence, since the cost price of a fast reactor depends on the lifetime of its components, the number of experiments carried out in this research field is steadily increasing, resulting in a large amount of data. There is still a need, however, for adequate theoretical models to explain the swelling phenomenon. Most experimental data on swelling reported up till now, are valid for neutron fluences far below the maximum dose, to which the structural components of a future fast reactor will be subjected. Since experimental swelling data are not available for doses in excess of 10^{23} n cm^{-2} ($E > 0.1$ MeV), theoretical expressions for the macroscopic swelling are required for making reliable extrapolations of existing data towards higher doses.

2. Pure metals

A summary of void formation data in pure metals as derived from transmission electron microscopic observations is given in tables 2A and 2B. From the average void diameter $\bar{d}$ and the void density ρ, the volume fraction of voids $\frac{\Delta V}{V}$ can be computed by means of the approximated expression $\frac{\Delta V}{V} = 0.5\,\rho\,\bar{d}^3$.

TABLE 2A

Void formation data in pure metals

Metal	Purity$^{(***)}$ (%)	Irradiation Temperature (°C)	$T/T_m$$^{(****)}$	Fluence × 10^{-19} (E > 1 MeV) (n cm^{-2})	Average void diameter (Å)	Void density × 10^{-14} (cm^{-3})	$\frac{\Delta V}{V}$ (%)
FCC - METALS							
Ni (3)	99.997	260	0.31	12	60	200	0.21
	99.997	380	0.38	5.7	83	40	0.11
	99.997	500	0.45	5.7	165	8	0.16
	99.997	575	0.49	6.2	245	2.5	0.17
Ni (4)	99.98	370-438	0.38-0.41	2(*)	(**)	(**)	(**)
Ni (40)	99.98	450	0.42	300(*)	400	1.8	0.64
Ni (45)	99.997	380	0.38	5	100	40	0.2
Cu (3)	99.999	260	0.39	12	230	3	0.17
Al (3)	99.999	50	0.35	3.2	270	(**)	(**)
Al (5)	99.	50	0.35	1 500	(**)	(**)	(**)
Al (5)	99.9999	50	0.35	35	(**)	1.3	(**)
Al (5)	99.	50	0.35	35	no voids observed		
Al (39)	99.9999	55	0.36	1 000(E > 0.82 MeV)	∿ 200	1.1	0.04
BCC - METALS							
V (6)	commercial	630	0.41	1 700(*)	100	>10	0.05
Mo (3)	99.99	800	0.37	3	65	100	0.12
Mo (7,46)	99.98	700	0.34	14	40	300	0.1
Mo (7,46)	99.98	1 000	0.44	13	200	5	0.19
Mo (8)	99.99	1 050	0.45	100(*)	290	1.2	0.17
Mo (8)	99.99	1 150	0.49	100(*)	470	0.5	0.28
Fe (4)	99.999	450	0.40	300(*)	280	1	0.12
W (33)	(**)	∿ 1 300	∿ 0.43	10	(**)	10	(**)
W (46)	99.992	1 000	0.35	15	37	200	0.04
	99.992	1 300	0.43	16	100	10	0.05
HCP - METALS							
Re (8)	99.97	1 050	0.38	100(*)	110	7	0.07
Re (8)	99.97	1 150	0.41	100(*)	470	5	0.10

(*) E > 0.1 MeV
(**) Not reported
(***) Metallic elements
(****) T = irradiation temperature (in K); T_m the melting point temperature (in K)

TABLE 2B

Temperature dependence of void formation in pure nickel (99.997 %) (3, 41, 43)

Irradiation Temperature °C	T/T_m	Fluence $\times 10^{-19}$ ($E > 1$ MeV) ($n\ cm^{-2}$)	Average void diameter (Å)	Void density $\times 10^{-14}$ (cm^{-3})	$\frac{\Delta V}{V}$ (%)
50	0.19	4.0	no voids observed		
260 (estimated)	0.31	12	60	200	0.21
380	0.38	5.2	83	40	0.11
500	0.45	5.7	165	8	0.16
575	0.49	6.2	245	2.5	0.17
640	0.53	5.2	270	0.8	0.07
750	0.59	5.2	∿ 400	∿ 0.001	<0.001

From table 2A the following general conclusions can be drawn.

a) Voids induced by fast neutron irradiation have been observed in three groups of metals belonging to the three most important crystal structures for metals, thus suggesting that void formation is a fast neutron radiation damage effect for metals in general. The situation for h.c.p. metals, however, is not quite clear. Indeed, no voids could be observed in highly pure zirconium nor in highly pure titanium (99.99 %) irradiated at 450°C [$0.39\ T_m$ (Zr); $0.42\ T_m$ (Ti)] up to a fluence of $3 \times 10^{21}\ n\ cm^{-2}$ ($E > 0.1$ MeV) (9).

b) For all metals thus far investigated (see tables 2A and 2B) one observes that the void diameter increases with irradiation temperature. The exact temperature dependence has been determined for nickel (see table 2B), which shows maximum swelling at 500°C ($0.45\ T_m$)

(43) for a fluence of 5.2×10^{19} n cm^{-2} (E > 1 MeV). It is estimated that no swelling occurs in nickel below 250°C ($\sim 0.3\ T_m$) nor above 700-750°C [see also (41)]. Bullough, Eyre and Perrin (10, 11) have shown theoretically that for annealed molybdenum the growth rate of a void is maximum around 900°C ($0.4\ T_m$). In this respect, the behaviour of pure metals is very similar to that of austenitic steels, where peak swelling occurs around 500°C ($0.4\ T_m$) (see § 3).

c) Fast neutron irradiation of pure metals results in void formation if the irradiation temperature is above $0.3\ T_m$, i.e. beyond the temperature at which vacancies become mobile (12, 13).

d) Among the several intrinsic properties of a particular metal, which may influence void formation and void growth, the most important ones are the crystallographic structure, the stacking fault energy, surface energy, migration energy of vacancies and melting point. For FCC metals, if the stacking fault energy is high, as it is the case for e.g. nickel ($\sim$ 300 erg/cm^2), the void will be the lowest energy form among the possible vacancy defect clusters (Frank loops, tetrahedra, voids) (50). This implies that voids will form in pure Ni at relatively low doses. The magnitude of the stacking fault energy compared to that of the surface energy may be used as a criterion for estimating the threshold dose for void formation in a particular metal, at least for FCC metals. It is in fact generally assumed that in order to obtain void growth their three-dimensional morphology must be gas stabilized. If neutronic gas is needed for this stabilization, the irradiation dose for the onset of void formation will be higher for metals with a lower stacking fault energy.

Once voids have been formed in a particular metal their growth rate will depend on the migration energy of vacancies, or, more exactly, on the ratio E_m^v/T_m where E_m^v = migration energy of vacancies, and T_m = melting point (in K). For the three FCC metals Al (E_m^v = 0.6 eV T_m = 933 K), Cu (E_m^v = 1.06 eV, T_m = 1 366 K), and Ni (E_m^v = 1.4 eV, T_m = 1 726 K) (14, 51) it turns out that

$$\frac{E_m^v}{T_m}\ (\mathrm{Al}) < \frac{E_m^v}{T_m}\ (\mathrm{Cu}) < \frac{E_m^v}{T_m}\ (\mathrm{Ni})$$

Since the diffusion rate of vacancies is proportional to exp $(- \frac{E_m^v}{\alpha k T_m})$, one may expect that voids will grow more rapidly in Al than in Cu and Ni, if the three metals are irradiated under the same conditions and at the same homologous temperature $T = \alpha T_m$ $(\alpha < 1)$ and if one assumes that the proportionality factor in the diffusion rate equation for vacancies is nearly the same for the three metals. The experimental data of table 2 seem to indicate such general trend for FCC metals. At comparable homologous irradiation temperatures, the mean diameter $\bar{d}$ of the voids seems to increase with decreasing ratio E_m^v/T_m : $\bar{d}$ (Ni) $\simeq$ 83 Å for $\alpha = 0.38$, $\bar{d}$ (Cu) $\simeq$ 230 Å for $\alpha = 0.39$ and $\bar{d}$ (Al) $\simeq$ 270 Å for $\alpha = 0.35$.

For BCC metals no exact data for the migration energy of vacancies are available. There is, however, some experimental evidence that E_m^v (Mo) $\simeq$ 2 eV (13, 14) and E_m^v (Fe) $\simeq$ 1.1 eV (14), which yields $\frac{E_m^v}{T_m}$ (Mo) > $\frac{E_m^v}{T_m}$ (Fe). At the same homologous irradiation temperature and under the same irradiation conditions voids will grow more rapidly in Fe than in Mo. This behaviour seems to be confirmed by the data of table 2 : 65 Å < $\bar{d}$ (Mo) < 200 Å for $0.37 < \alpha < 0.44$, d (Fe) $\simeq$ 280 Å for $\alpha \sim 0.40$. For HCP metals, the available data are insufficient to check the validity of this rule.

e) The influence of impurities is not quite clear. However, the general trend can be derived from the following reasoning. Stiegler et al (5) have observed that voids did not form in low purity (99 %) Al at a dose of 3.5×10^{21} n cm^{-2} at 50°C, whereas voids could be observed in highly pure (99.9999 %) Al irradiated under the same conditions. The lower purity Al had to be irradiated to a dose of 1.5×10^{22} n cm^{-2} before voids could be observed. Similarly, voids have been observed in commercially pure vanadium after a dose of 1.7×10^{22} n cm^{-2} at 630°C, but not in a V-20 % Ti alloy irradiated under the same conditions (15). In pure iron, voids form at fluences of about 10^{21} n cm^{-2} whereas in iron alloys voids are only observed after irradiation to fluences in excess of 10^{22} n cm^{-2}. These observations indicate that the threshold fluence, i.e. the minimum dose at a given temperature at which voids form, decreases with increasing purity of the metal. It is rather unexpected that voids form in pure metals at such low doses where the total neutronic gas concentration is still too low to efficiently stabilize the void nuclei, whereas, on the other hand, they form only at much higher doses in impure metals and alloys where the neutronic gas content is much higher. At first sight, this seems to be in contradiction with the swelling model, following which void nuclei have necessarily to be gas stabilized in order to insure their three-dimensional morphology and growth. However, it may be that dissolved gases in pure metals play an important rôle in the stabilization of void nuclei. It is known in fact that after zone refining the concentration of dissolved gases may remain relatively high. In impure metals (and alloys) these dissolved gases may be gettered by the impurities during preparation. If it are the dissolved gas atoms which stabilize the void nuclei in pure metals at low doses, and, if it are the dissolved neutronic gas atoms (mainly helium as a consequence of the high mobility of hydrogen at the usual irradiation temperatures) which take over the stabilizing rôle in impure metals and alloys at corresponding higher doses, than the difference in swelling behaviour between pure metals and impure metals (alloys) can be readily explained.

This difference in behaviour may be a justification for research on the swelling of pure metals. Since in pure metals swelling occurs at rather low doses, swelling data can be become available in shorter time and in a larger dose range than it is presently the case for alloys. Questions such as (i) the percentage volume increase at which saturation of swelling occurs (ii) the influence of alloy composition on the amount of swelling (iii) the influence of alloy prehistory, etc... cannot be solved presently for a particular alloy as a consequence of e.g. too high doses at which the saturation phenomenon occurs, too complicated alloy structures and insufficiently controlled irradiation conditions. Research on pure metals may be helpful to understand the basic mechanism underlying the swelling phenomenon of alloys.

Kulcinsky et al.(40) have made a detailed study of the annealing behaviour of voids in pure nickel after irradiation at 450°C to 3×10^{21} n cm^{-2} ($E > 0.1$ MeV). They observed that the voids in the center of the grains did not coarsen during annealing. The average size remained at ∿ 400 Å up to the temperature of complete annealing (1 050°C). This behaviour is different from that in austenitic steels, where such void coarsening during annealing has been observed [see table V and (35, 38)]. It is also in contradiction with a similar study made by Brimhall and Mastel (41). These authors found that all voids produced in pure nickel during irradiation to a fluence of 1×10^{20} n cm^{-2} ($E > 0.1$ MeV) disappeared at 800°C. Furthermore, the average void size increased with increasing annealing temperature. Kulcinski et al. believe that their observations have to be explained on the basis of a different neutronically produced helium content in their specimens (∿ 30 times more than in the specimens of Brimhall and Mastel). Therefore, the voids in their study are believed to be partially gas-filled cavities. Bullough and Perin (42) have developed an annealing theory for such gas-filled cavities, which indicates (40) that the thermal stability of the cavities increases and that their average size remains relatively constant.

3. Alloys

3.1. Austenitic Stainless Steel

Whereas the study of the swelling phenomenon in pure metals can be very helpful in understanding the swelling mechanism, most effort has of course been paid to collect experimental data on the swelling of candidate alloys for the construction of fast reactor components. Among the various alloys, the austenitic steels 304 and 316 have been studied in most detail. For these alloys the available experimental data are to be found in the temperature range 350 - 750°C for integrated doses up to ∿ 10^{23} n cm^{-2} ($E > 0.1$ MeV). The maximum swelling occurs at about 500°C and amounts to about 7 % at

7×10^{22} n cm^{-2}. It is estimated that no swelling occurs below 350°C nor above 750°C (see table III).

Lauritzen et al (22, 23) and Bloom and Stiegler (20) have shown that minor changes in alloy composition can significantly reduce the amount of swelling. Type 304 steel shows twice the swelling effect of type 347 steel (22, 23) (see table III) after irradiation under the same conditions.

TABLE III

Summary of the swelling data for austenitic steels

Material	Irradiation temperature* (°C)	Fast neutron dose (E > 0.1 MeV) $\times 10^{-22}$ (n cm^{-2})	Total void volume (%)	Volume increase $\frac{\Delta V}{V}$ (%)
316 (2)	450	5.2 (a)	0.8	-
	500	7.8 (a)	7	7
	510	4.5 (a)	1.5	-
	560	3.2 (a)	0.2	-
316 AR (16)	955	2.4		0.03
316 AR (16)	770	2.4		0.29
316 SA (16)	955	2.4		0.36
316 SA (16)	770	2.4		0.61
316 AR (16)	955	2.4		0.30
316 AR (16)	770	2.4		0.13
304 AR (16)	955	2.4		- 0.16
				0.29
304 A (17)	370	0.601		0.11 (0.14)(b)
		0.83		0.14 (0.19)
		0.88		0.12 (0.22)
		1.08		0.29 (0.44)

	1.19		0.36 (0.28)
	1.19		0.36 (0.25)
	1.25		0.29 (0.31)
	1.34		0.27 (0.30)
	1.50		0.24 (0.37)
	2.00		0.53 (0.68)
	2.00		0.37 (0.82)
	2.15		0.47 (0.92)
	2.33		0.41 (0.52)
	2.62		0.47 (0.59)
	2.66		0.54 (1.09)
	2.92		0.51 (0.72)
	2.98		0.96 (0.70)
	4.34		0.93 (0.98)
	5.34		1.55 (1.20)
380	2.96		0.44 (1.27)
	3.08		1.13 (1.27)
	3.16		0.80 (1.30)
	5.57		0.87 (1.25)
	6.14		1.53 (1.38)
	6.25		2.44 (1.40)
385	5.91		0.63 (1.40)
390	3.41		1.27 (1.40)
	6.40		2.41 (1.44)
	6.75		3.09 (1.52)
395	6.75		2.63 (1.61)
400	1.92		0.13 (1.4)
	3.16		1.35 (1.30)
	3.50		1.15 (0.87)
	5.89		3.09 (1.32)
	6.25		2.41 (1.40)
405	6.45		3.70 (1.52)
410	3.76		1.26 (1.28)
420	2.25		0.27 (1.66)

	2.54		1.35 (1.04)
	2.54		1.42 (1.04)
	2.66		0.92 (1.09)
	4.80		2.44 (1.08)
	4.89		1.85 (1.15)
	5.33		1.53 (1.20)
	6.47		4.10 (1.36)
430	2.00		0.47 (0.82)
	2.26		0.88 (0.56)
	3.46		1.55 (0.776)
	3.54		0.95 (1.52)
	4.34		0.87 (0.98)
440	1.58		0.31 (0.39)
	2.25		0.33 (1.66)
	2.62		0.93 (0.590)
	3.39		1.42 (1.40)
	3.39		1.95 (1.40)
	4.88		2.48 (1.02)
450	0.66		0.13 (0.99)
	1.08		0.22 (0.44)
	1.10		0.34 (0.81)
	1.28		0.41 (0.288)
	2.33		0.47 (0.52)
	3.42		1.67 (1.16)
460	0.07		0.05 (0.01)
	0.18		0.05 (0.04)
	0.29		0.05 (0.07)
	0.45		0.15 (0.18)
	0.51		0.06 (0.12)
	0.73		0.19 (0.18)
	0.92		0.27 (0.20)
	2.27		0.92 (0.47)
	2.69		1.11 (1.27)

		3.24		2.06 (1.33)
	470	0.006		0.04 (0.002)
		0.05		0.06 (0.02)
		0.18		0.12 (0.077)
		0.19		0.05 (0.07)
		0.25		0.11 (0.06)
		0.30		0.54 (0.06)
		0.36		0.14 (0.081)
		0.81		0.10 (0.34)
		2.24		2.09 (1.04)
		2.58		1.15 (0.87)
	480	0.83		0.06 (0.28)
		1.67		0.28 (0.59)
		2.24		1.43 (1.04)
	490	0.88		0.29 (0.36)
304 A (18)	370	2.00		0.37
		2.66		0.54
		2.80		0.70
		3.00		0.47
		3.20		0.50
		4.60		1.05
	371	5.30		1.86
	372	5.57		0.87
	374	6.10		0.60
	377	6.14		1.53
		6.20		2.68
	380	3.16		0.80
	387	6.40		2.60
	388	6.40		2.41
	390	3.41		1.27
	394	6.40		1.30
	396	6.20		3.35

	400	3.16		1.35
	403	5.89		3.09
	405	6.20		3.20
	407	5.60		3.70
	415	5.20		3.07
	420	2.66		0.92
		4.80		2.44
	426	3.80		1.90
	427	5.60		4.10
	430	5.60		1.72
	433	3.46		1.55
	441	2.62		0.93
		2.70		0.96
	444	3.80		2.50
316 ST (18)	518	1.26		0.30
	562	1.26		0.32
	621	1.98		0.59
	671	1.98		0.32
	679	2.88		0.66
	743	2.88		0.28
304 L (19)	370	0.8		0.07
	398	1.2		0.15
	438	1.4		0.17
	465	1.3		0.16
	472	0.9		0.08
304 (20)	450 ± 50	1.75		0.57
304L(c)(20)	450 ± 50	1.53		0.14
304 A (21)	375	2.4	0.13	0.53
	410	4.5	0.21	1.26
	450	4.1	0.34	1.67
	463	3.1	1.06	1.15
		2.4	0.43	(d)

		2.0	(d)	0.28
		1.0	(d)	0.06
304 A (22)(23)	660	3.4	1.1	1.21
347 A (22)(23)	660	3.4	0.08	0.54
Incoloy 800 A(22)(23)	660	3.4	2	2.47
304 (24)	371	2.9		0.47
		1.4		0.36
	380	4.2		0.44
	382	7.0		0.33
	395	10.0		2.63
	405	9.1		3.70
	408	10.0		1.34
	420	5.5		1.85
	425	9.1		4.14
	430	5.0		0.95
	440	5.5		2.48
	460	3.8		1.11
	463	1.8		0.93
	470	0.12		-
		0.31		0.12
		1.2		0.10
	474	0.9		0.54
304 L (44)	373 (e)	1.2		0.12 ± 0.04
	373	1.7		0.29 ± 0.03
	373	2.8		0.24 ± 0.03
	386	4.0		0.51 ± 0.04
	422	4.8		1.15 ± 0.03
	463	3.1		0.88 ± 0.03
	463	2.2		0.31 ± 0.03
	463	1.0		0.19 ± 0.03

	463	0.7		0.06 ± 0.03
	463	0.4		0.05 ± 0.03
	463	0.25		0.05 ± 0.03
	463	0.10		0.05 ± 0.03
	404	1.9		0.13 ± 0.05
	419	2.3		0.27 ± 0.05
	430	2.3		0.33 ± 0.05
	448	1.3		0.34 ± 0.05
	451	0.8		0.13 ± 0.04

(a) Total neutron dose

(b) Number between brackets represents the value of the flux in 10^{15} n cm^{-2} s^{-1} (E > 0.1 MeV)

(c) Titanium modified type 304 L stainless steel

(d) Not measured

(e) Calculated temperatures

A Means mill annealed condition

AR Means as received

SA Means solution annealed at 1 200°C/24 h

ST Means solution treated

* Mostly estimated values

Even a larger reduction of swelling has been reported for titanium-modified type 304 L stainless steel with respect to standard type 304 stainless steel (20) (see table III).

Since experimental swelling data are available for doses up to 10^{23} n cm^{-2} only (see table III) one tries to estimate the amount of swelling at higher doses by extrapolating curves which are based either on theoretical swelling models or on empirical relations, both fitting sufficiently well to the experimental data in the lower dose range.

On the basis of immersion density measurements made in several laboratories (PNL, ANL, GE) on a large number of type 304 specimens taken from EBR-II components in the dose range $0.005\ 10^{22}$ - $6.75\ 10^{22}$ n cm^{-2} (E > 0.1 MeV) and irradiation temperature range 370°C - 490°C (see table III) Claudson et al (17) have derived the following empirical relation between volume change $\frac{\Delta V}{V}$ (%), fast neutron dose Φ t (n cm^{-2}) and irradiation temperature T (K) for austenitic stainless steel type 304 :

$$\frac{\Delta V}{V} = 1.05 \times 10^{-34} (\Phi\ t)^{1.65} \exp. \frac{-10,200}{RT} \qquad (1)$$

Another empirical relation based on similar data has been proposed by Claudson and Barker (25) for annealed 304 austenitic steel:

$$\frac{\Delta V}{V} = 5.0 \times 10^{-36} (\Phi\ t)^{1.66} [\exp (- 6800/RT) -1.87 \times 10^4 \exp (-27,000/RT)] \qquad (2)$$

A later analysis (18) of EBR-II data, including ORNL data on EBR-II specimens and including PNL data on mechanical property type 316 specimens (see table III) irradiated in the temperature range 518-743°C and dose range $1.26 - 2.88 \times 10^{22}$ n cm^{-2}, yields for austenitic stainless steel type 304 and 316 the following empirical relation :

$$\frac{\Delta V}{V} = 10^{-48.31} \times (\Phi\ t)^{1.71} \times 10^{\left(\frac{1.55 \times 10^4}{T} - \frac{5.99 \times 10^6}{T^2}\right)} \qquad (3)$$

This expression results in a $(\frac{\Delta V}{V}, T)$ curve which according to the authors fits very well to the experimental data at $5 \cdot 10^{22}$ n cm^{-2} (E > 0.1 MeV). By this equation a maximum swelling of 3.4 % is predicted at 500°C and at 5×10^{22} n cm^{-2} (E > 0.1 MeV). It is further estimated by the authors that no swelling occurs above 750°C, although the empirical curve at $5 \cdot 10^{22}$ n cm^{-2} predicts a volume increase of about 1 % at that temperature.

Recently (24) Claudson has proposed a few other emperical equations, based on bulk density measurements and on a thorough analysis of the defect structure (void size, void density and dislocation loop structure) of austenitic stainless steel after irradiation in EBR-II in the temperature range 460-600°C and fluence range $4 \times 10^{21} - 6 \times 10^{22}$ n cm^{-2} (E > 0.1 MeV). For solution treated 304 and 316 stainless steel the following empirical equation is proposed:

$$\frac{\Delta V}{V} = (\phi t)^{2.05-27/\Theta+78/\Theta^2} \times \left[(T-40)\times 10^{-10}\right] \times \exp\left[-0.015\ T - 5100/T + 32.6\right] \tag{4}$$

where Φ t = neutron fluence (n cm^{-2} × 10^{-22}, E > 0.1 MeV)

Θ = T - 623

T = absolute temperature (K)

A similar analysis for cold-worked austenitic steel yields :

$$\frac{\Delta V}{V} = 10^{-36.0} \times (\phi t)^{1.69}\left[\exp(-7808/RT) - 5480 \exp(-25{,}300/RT)\right] \tag{5}$$

where Φ t = fast neutron fluence (n cm^{-2}, E > 0.1 MeV)

R = gas constant

T = absolute temperature (K)

Another empirical equation relating swelling to irradiation temperature and fluence has been proposed (16), assuming a beta distribution for the experimental data with a lower temperature threshold for swelling estimated at 360°C and an upper limit at 775°C. This equation reads as follows :

$$\frac{\Delta V}{V} = 3.14\ (10^{-4})\ (F)^{1.81}\ (T - 360)^{0.683}\ (775 - T)^{0.577} \tag{6}$$

F = fast fluence /10^{22} n cm^{-2} (E > 0.1 MeV)

T = irradiation temperature (°C)

The swelling of stainless steel 304 and 316 as predicted by these empirical equations is shown on fig. 1, for doses up to 3.10^{23} n cm^{-2} (E > 0.1 MeV).

From fig. 1 one can derive the following conclusions.

a. The empirical equations predict $\frac{\Delta V}{V}$ - values which become physically unrealistic for doses beyond 10^{23} n cm^{-2}. At lower doses the correspondence between measured and empirically derived values is satisfactory. Therefore, the above-mentioned empirical relations should only be used for interpolation below 10^{23} and not for extrapolation beyond this dose. The reason for this is that apart from some mathematical objections, the largest part of the available data lie in too narrow a dose interval below 10^{23} n cm^{2} (between 10^{22} and 6.10^{22} n cm^{-2} only a few data are available at 10^{23} n cm^{-2}, see table III) so that a reliable extrapolation of $\frac{\Delta V}{V}$ beyond 10^{23} n cm^{-2} cannot be expected. Furthermore, the influence of swelling saturation, due to the interaction between radiation induced extended defects, on the extrapolated values cannot be estimated since the empirical equations are based on data which themselves do not reflect such saturation.

   The most reliable empirical equation presently available seems to be equation 3, since it is based on a range of data which is most extended with respect to both dose and temperature. Table IV gives low dose numerical data for annealed austenitic stainless steel type AISI 304 and 316 as calculated by means of this equation.

b. Austenitic stainless steels type 304 and 316 show peak swelling around 500°C in the annealed condition, whereas peak swelling is shifted towards higher temperatures (620°C) for cold-worked material. At first sight, an enhanced dislocation concentration seems to reduce the amount of peak swelling and to delay swelling with respect to temperature. This effect may cause swelling saturation, even for annealed material, since neutron irradiation increases the dislocation concentration continuously. At high doses, the dislocation concentration (network of intersecting loops) becomes comparable to that of cold-worked material.

TABLE IV

Numerical swelling data calculated by means of equation (3) for annealed austenitic stainless steel type AISI 304 and 316 (E_m > 0.1 MeV)

T (°C)	ΔV/V (%)		
	10^{22} n cm^{-2}	5.10^{22} n cm^{-2}	10.10^{22} n cm^{-2}
350	0.057	0.895	2.928
400	0.131	2.048	6.701
450	0.195	3.052	9.984
500	0.213	3.407	11.145
550	0.199	3.127	10.231
600	0.160	2.515	8.228
650	0.118	1.850	6.052
700	0.082	1.283	4.198

c. Results obtained by Holmes (44) on austenitic stainless steel type 304 L show a linear relationship between $\frac{\Delta V}{V}$ and fluence in a double logarithmic diagram (see table III), when one subtracts a dose independent residual volume change, observed at low doses (< 5.10^{21} n cm^{-2}). It turns out that $\frac{\Delta V}{V} \sim (\text{dose})^{1.7 \pm 0.2}$ for 304 L austenitic steel which compares very well to empirical equation (3) valid for type 304 and 316 steel. Holmes data yield extrapolated $\frac{\Delta V}{V}$ - values between 3 % and 6 % at 10^{23} n cm^{-2} at the mean irradiation temperature (∿ 420°C see table III for temperature data).

Harkness et al.(26 - 28) have developed theoretical models for explaining the experimentally observed swelling effects in austenitic steels. Fig. 2 and 3 show the theoretically expected void volumes (%) as a function of irradiation temperatures and dose for different models : (i) a simple void nucleation and void growth model (26) (ii) void nucleation-growth model combined with saturation effects due to an increased sink density (voids, dislocation loops). This theory predicts a linear relationship between swelling and dose whereas empirically higher power relations between swelling and dose have been deduced (see fig.4). If saturation is taken into account, theory predicts a maximum swelling of 14 % occurring at 490°C at 3.10^{23} n cm^{-2}. This theoretical prediction is in agreement with predictions on swelling saturation made by Straalsund and Holmes (29). On the basis of considerations on void-interstitial loop interactions, these authors predict that swelling should be saturated at 5 to 20 % swelling. An extrapolation of experimental data for EBR-II components (austenitic steel type AISI 304) yields a swelling of less than 20 % at 3.10^{23} n cm^{-2} (see table III).

Bullough et al.(10, 11) and Bullough and Perrin (30, 31) have made a theoretical study of the swelling phenomena, using a surface step model for the trapping of point defects at the surface of the void. This study shows that voids are first nucleated as three-dimensional vacancy-inert gas atom clusters (small gas bubbles). The presence of gas in these nuclei is believed to be necessary for their further growing as three-dimensional clusters. Without gas, vacancy clusters would take a two-dimensional form and no swelling would occur. Indeed, during growth as a consequence of further vacancy absorption, these nuclei will keep their two-dimensional form. The above-mentioned authors have also studied the influence of cold-work on the amount of swelling. Their theory predicts that a high dislocation density substantially decreases the amount of swelling at low doses, but that at high doses the swelling is more pronounced than in low dislocation density material at equivalent doses. This is in agreement with the empirical equations (4) and (5) which predict a reduction of swelling by a factor of about

2 at doses below 10^{23} n cm^{-2}.

Foreman (47) has published some comments on the theory of Bullough and Perrin (42, 48). Assuming that around a void a denuded zone is created and that the steady-state concentration of point defects is independent from the void size, Foreman shows, along the lines of a void growth theory proposed by Greenwood et al.(49), that $\Delta V \sim (\text{dose})^{3/2}$ instead of $\Delta V \sim (\text{dose})^3$ as predicted by the theory of Bullough and Perrin. The result of Foreman is in better agreement with the dose dependence predicted by Harkness et al.($\Delta V \sim$ dose (28)) and the experimental results on austenitic steels ($\Delta V \sim \text{dose}^{1.7 \pm 0.2}$(44, 18)). Furthermore, the deleterious effect of cold-work on swelling at high doses as predicted by Bullough and Perrin (11)* is not expected by the volume diffusion theory of Greenwood et al.(under the assumption that voids are perfect sinks for point defects). The latter theory predicts a marked reduction in void growth, if the dislocation density is increased from 10^{10}lines/cm^2 to 10^{12} lines/cm^2 provided that the void density is not increased too much (due to new nucleation centres).

Holmes et al.(35) report on the annealing behaviour of voids in 304 stainless steel. The data are summarized in table V.

---

*This theory predicts a lower swelling at low doses but a much higher swelling at high doses for cold-worked material as compared to annealed material.

TABLE V

Defect densities and sizes in types 304 stainless steel after irradiation to 1.4×10^{22} n cm^{-2} (E > 0.18 MeV) (35)

Post-irradiation annealing temperature (°C)	Voids	
	Average size (10^{-6} cm)	Density (10^{14} cm^{-3})
Initial (532°C)	1.6 ± 0.4	4.9 ± 2.1
482	2.3 ± 0.2	1.9 ± 0.3
593	2.2 ± 0.5	1.9 ± 0.5
648	2.7 ± 0.2	1.2 ± 0.2
704	2.5	1.7
760	2.3 ± 0.1	0.5 ± 0.2
816	2.6	0.01
871	none found	none found

From this table it can be concluded that during post-irradiation annealing, the average void size increases and that the void density decreases. After heating at 870°C all voids have disappeared. This is quantitatively confirmed by a post-irradiation annealing study on type 304 L stainless steel made by Stiegler and Bloom (38).

Since the study of the annealing of voids is performed by means of the TEM-technique care should be taken in evaluating the "average void diameters" which are given by different investigators. It has been found (36) that the distribution of voids in irradiated 304 L stainless steel depends on the thickness of the foil. For decreasing foil thickness, the number of the large voids per cm^3 is decreased, whereas for increasing foil thickness the number of small voids per cm^3 is decreased.

3.2. Other alloys

The low fluence swelling behaviour of three commercial nickel alloys has been investigated by Holmes (32). The data are shown on fig. 5. Specimens of Nickel-270 (99.98 % Ni) Nickel-200 (99.6 % Ni) and Inconel-600 (73 % Ni, 17 % Cr, 8 % Fe) in the annealed and 50 % cold-worked condition, were irradiated in EBR-II to a total peak fluence of about 4.3×10^{22} n/cm^2 at $\sim$ 450°C. Various fluence levels could be obtained due to the flux gradient in EBR-II. The effect of purity is clear, and consistent with irradiation studies on pure nickel (see table II). There is no effect of 50 % cold-working on the amount of swelling. In this study, inconel-600 showed a volume decrease in the total dose range, this is also the case for Ni-200 at low doses. The reason for this decrease is not well understood. Fig. 5 clearly shows the marked difference between the swelling kinetics for nickel-alloys and austenitic steels. The threshold fluence to initiate swelling is less than 10^{20} n cm^{-2} ($E > 0.1$ MeV) for nickel-alloys, while for austenitic steels the threshold is near to 10^{22} n cm^{-2}. This difference can be related to the difference in stacking fault energy between nickel alloys and austenitic steels. The nickel alloys with a high nickel content have a high stacking fault energy as it is the case for pure nickel. The stacking fault energy of inconel-600 (low nickel content) will be comparable to that of austenitic steel. Therefore, at equal dose and temperature, $\frac{\Delta V}{V}$ (Ni-270) > $\frac{\Delta V}{V}$ (Ni-200)> $\frac{\Delta V}{V}$ (Inconel-600). Another difference between the swelling behaviour of nickel-alloys and austenitic steels is to be found in the fact that there exists evidently a linear relationship between swelling and dose in the former case whereas in the latter case theory predicts such a linear relationship but the empirical relations point to a higher power law (see fig. 4).

C.D. Williams and R.W. Gilbert report (34) that no three-dimensional voids could be observed either in zircaloy-2 irradiated to doses in excess of 10^{21} n cm^{-2} at about 300°C or in similar material irradiated in the DFR to a fluence of about 4×10^{21} n cm^{-2} at about 500°C. King et al (37) have studied a cold-drawn Al- 1 % Ni alloy (Al-8 001, i.e. 1 100 grade Al with 1 % Ni addition) after irradiation at 60°C to 1×10^{22} fast neutrons/cm^2 ($E > 0.8$ MeV) and to a thermal

dose in excess of 2 × 10^{22} thermal neutrons/cm^2. The specimens contained polyhedral voids, ranging in diameter up to 550 Å at a concentration of ∿ 1 × $10^{15}/cm^3$. Additional doping of the specimens in a thermal flux before fast neutron irradiation decreased the maximum diameter to about 300 Å but increased the concentration to about 2 × $10^{15}/cm^3$. Apart from the voids, a fine solid precipitate of silicon produced by the ^{27}Al (n, γ) reaction followed by beta decay to ^{28}Si, was observed. The swelling caused by the observed voids was calculated to be ∿ 0.4 % (with doping) and 0.8 % (without doping). Upon-annealing at temperatures above 220°C the voids disappeared and the irradiation-produced precipitate coarsened. As a result of irradiation, the recrystallization temperature of the cold-worked material increased from 200°C to over 500°C. This large increase is believed to be due to the formation of bubbles on grain boundaries and precipitate matrix interfaces.
Bubbles were observed after annealing at 400°C and their growth on annealing at ∿ 530°C caused significant swelling (7 % to 10 %). The annealing behaviour of the voids is a direct indication that they are partially filled with gas (not equilibrium gas bubbles) since gas bubbles (cavities containing gas at the Laplace pressure) are believed to remain unaltered or to coarsen during low temperature annealing.

4. Conclusion

Although a large amount of experimental and theoretical data on the swelling behaviour of metals and alloys has been published in recent years, a number of points remain to be clarified. The most important are :

(1) the influence of changes of microstructure (dislocation density,grain size, precipitates,...), purity and alloy composition on the swelling of a particular alloy (temperature and amount of peak swelling, threshold dose, swelling saturation,...);

(2) the influence of intrinsic parameters such as stacking fault energy,

surface energy, crystallographic structure (e.g. austenitic steel, ferritic steel) on the swelling parameters;

(3) the reduction of swelling by periodic in situ annealing;

(4) the dose level at which swelling should saturate. Theory predicts that in austenitic steel 304 and 316 swelling should saturate at $\frac{\Delta V}{V} = 12$ %. This could not be confirmed experimentally up till now, due to lack of data in the high dose range (> 10^{23} n cm^{-2}). The experimental data suggest saturation below $\frac{\Delta V}{V} \simeq 20$ %.

Since alloys seem to be rather complicated structures to study the swelling mechanism and since the experimental data show that pure metals behave quite similarly as far as swelling is concerned, a basic study of the swelling behaviour of pure metals could be very helpful in understanding the swelling mechanism. Such a study can be recommended the more so as the threshold dose for swelling for most pure metals is a few orders of magnitude lower than for most alloys.

Acknowledgement

The author thanks Dr J. Nihoul for stimulating discussions and for reading the manuscript.

References

(1) C. CAWTHORNE and E.J. FULTON
AERE-R 5269 (1966), 446-459

(2) C. CAWTHORNE and E.J. FULTON
Nature 216, 575 (1967)

(3) J.L. BRIMHALL and B. MASTEL
J. Nucl. Mat. 29, 123-125 (1969)

(4) G.L. KULCINSKI, B. MASTEL and J.L. BRIMHALL
Rad. effects 2, 57-59 (1969)

(5) J.O. STIEGLER, K. FARRELL, C.K.H. DUBOSE and R.T. KING
IAEA Symposium on Radiation Damage in Reactor Materials
Vienna, June 2-6, vol. II, 215-232 (1969)

(6) F.W. WIFFEN and J.O. STIEGLER
J. Met. 117A, (1968)

(7) J. MOTEFF, R.C. RAU and F.D. KINGSBURY
IAEA Symposium on Radiation Damage in Reactor Materials
Vienna, June 2-6, vol. II, 269-281 (1969)

(8) G.L. KULCINSKI, B. MASTEL and J.L. BRIMHALL
Trans ANS 13, 162, (1970)

(9) G.L. KULCINSKI
IAEA Symposium on Radiation Damage in Reactor Materials
Vienna, June 2-6, 247 (1969)

(10) R. BULLOUGH, B.L. EYRE, R.C. PERRIN
AERE-R6284 (1969)

(11) R. BULLOUGH, B.L. EYRE and R.C. PERRIN
Nucl. Appl. & Techn. 9, 346 (1970)

(12) J. NIHOUL
IAEA Symposium on Radiation Damage in Reactor Materials
Vienna, June 2-6, [illegible] (1969)

(13) L. STALS and J. NIHOUL
Physica 43, 678 (1969)

(14) J. DIEHL, D. SCHUMACHER, W. SCHILLING and A. SEEGER
Proc. Intern. Conf. Vacancies and Interstitials in Metals
Julich 23-28, Sept. 1968

(15) ANL, Reactor Development Program Progress Report
Sept. 1968
USAEC Rep. ANL-7500, p.100, Oct. 29, 1968

(16) GEAP-10028-32, p. 10-3

(17) T.T. CLAUDSON, J.J. HOLMES, J.L. STRAALSUND, H.R. BRAGER
IAEA Symposium on Radiation Damage in Reactor Materials
Vienna, June 2-6, 165 (1969)

(18) T.T. CLAUDSON, R.W. BARKER, R.L. FISH
Nucl. Appl. & Techn. 9, 10 (1970)

(19) J.O. STIEGLER, E.E. BLOOM, J.R. WEIR
Trans. ANS 11, 146 (1968)

(20) E.E. BLOOM and J.O. STIEGLER
J. Nucl. Mat. 35, 244 (1970)

(21) R. CARLANDER, S.O. HARKNESS and F.L. YAGGEE
Nucl. Appl. & Techn. 7, 67 (1969)

(22) T. LAURITZEN, A. WITHOP and U.E. WOLFF
Nucl. Eng. and Design 9, 265 (1969)

(23) U.E. WOLFF, A. WITHOP and T.A. LAURITZEN
Trans. ANS 12, 114 (1969)

(24) T.T. CLAUDSON
ANS Meeting Sept. 1970 Germany (Karlsruhe)

(25) T.T. CLAUDSON and R.W. BARKER
Trans. ANS 12, 523 (1969)

(26) S.D. HARKNESS and CHE-YU LI
IAEA Symposium on Radiation Damage in Reactor Materials
Vienna 2-6 June 1969, p. 189 vol. II

(27) S.D. HARKNESS
ANL-7595, July 1969

(28) S.D. HARKNESS, J.A. TESK, CHE-YU LI
Nucl. Appl. & Techn. 9, 24 (1970)

(29) J.L. STRAALSUND, J.J. HOLMES
Trans. Ans 12, 115 (1969)

(30) R. BULLOUGH and R.C. PERRIN
AERE T.P. 405, May 1970

(31) R. BULLOUGH and R.C. PERRIN
IAEA Symposium on Radiation Damage in Reactor Materials
vol. II, p. 233, Vienna June 2-6, 1969

(32) H.H. HOLMES
Trans. ANS 12, 117 (1969)

(33) J. MOTEFF
IAEA Symposium on Radiation Damage in Reactor Materials
Vienna 2-6 June 1969, p. 257, vol. II

(34) C.D. WILLIAMS, R.W. GILBERT
IAEA Symposium on Radiation Damage in Reactor Materials
Vienna 2-6 June 1969, vol. I, p. 235-247

(35) J.J. HOLMES, R.E. ROBBINS, J.L. BRIMHALL, B. MASTEL
Acta Met. 16, 955-967 (1968)

(36) A.L. BEMENT, G.J. BAU, E.A. EVANS, R.E. NIGHTINGALE
USAEC Report BNWL-919, November 1968

(37) R.T. KING, E.L. LONG, J.O. STIEGLER, K. FARRELL
J. Nucl. Mat. 35, 231-243, 1970

(38) J.O. STIEGLER and E.E. BLOOM
J. Nucl. Mat. 33, 173-185, 1969

(39) N.H. PACKAN and D.N. BRASKI
J. Nucl. Mat. 34, 307-314, 1970

(40) G.L. KULCINSKI, B. MASTEL, H.E. KISSINGER
Acta Met. 19, 27-36, 1971

(41) J.L. BRIMHALL and B. MASTEL
J. Nucl. Mat. 33, 189 (1969)

(42) R. BULLOUGH and R.C. PERRIN
IAEA Symposium on Radiation Damage in Reactor Materials
vol.II, p. 233 (1969)

(43) J.L. BRIMHALL and B. MASTEL
Scripta Met. 4, 51-54 (1970)

(44) J.J. HOLMES
J. Nucl. Mat. 29, 241-243 (1969)

(45) B. MASTEL and J.L. BRIMHALL
J. Nucl. Mat. 28, 115-117 (1968)

(46) R.C. RAU, R.L. LADD and J. MOTEFF
J. Nucl. Mat. 33, 324-327 (1969)

(47) A.J.E. FOREMAN
AERE-R 6358 (1970)

(48) R. BULLOUGH
AERE Report T.P. 375 (1969)

(49) G.W. GREENWOOD, A.J.A. FOREMAN, D.E. RIMMER
J. Nucl. Mat. 4, 305 (1959)

(50) J.A. SIGLER and D. KUHLMANN - WILSDORF
Phys. Stat. Sol. 21, 545 (1967)

(51) J. POLAK
Phys. Stat. Sol. 40, 677 (1970)

Captions for Figures

Fig. 1 a Swelling of annealed austenitic stainless steel AISI type 304, according to the empirical relation [eq. 1 (17)]

$$\frac{\Delta V}{V} (\%) = 1.05 \times 10^{-34} (\Phi t)^{1.65} \exp \frac{-10{,}200}{RT}$$

as a function of temperature and fast neutron fluence (the symbols are explained in the text).

Fig. 1 b Swelling of annealed austenitic stainless steel AISI type 304, according to the empirical relation [eq. 2 (25)]

$$\frac{\Delta V}{V} = 5.0\times10^{-36}(\Phi t)^{1.66} \exp[(-6800/RT)-1.87\times10^{4}\exp(-27{,}000/RT]$$

as a function of temperature and fast neutron fluence (the symbols are explained in the text).

Fig. 1 c Swelling of annealed austenitic stainless steel AISI type 304 and 316 according to the empirical relation [eq. 3 (18)]

$$\frac{\Delta V}{V} = 10^{-48.31}\times (\Phi t)^{1.71}\times 10^{\left(\frac{1.55\times10^{4}}{T} - \frac{5.99\times10^{6}}{T^{2}}\right)}$$

as a function of temperature and fast neutron fluence (the symbols are explained in the text).

Fig. 1 d Swelling of solution-treated stainless steel AISI type 304 and 316 according to the empirical relation [eq. 4 (24)]

$$\frac{\Delta V}{V} = (\Phi t)^{2.05-27/\theta + 78/\theta^{2}} \times [(T-40)\times10^{-10}]$$

as a function of temperature and fast neutron fluence (the symbols are explained in the text).

Fig. 1 e Swelling of cold-worked stainless steel AISI type 304 and 316 according to the empirical relation [eq. 5 (24)]

$$\frac{\Delta V}{V} = 10^{-36.0} \times (\Phi t)^{1.69}[\exp(-7808/RT)-5480 \exp(-25,300/RT)]$$

as a function of temperature and fast neutron fluence (the symbols are explained in the text).

Fig. 1 f Swelling of austenitic stainless steel AISI type 304 and 316 according to the empirical relation [eq. 6 (16)]

$$\frac{\Delta V}{V} = 3.14\ (10^{-4})(F)^{1.81}(T-360)^{0.683}(775-T)^{0.577}$$

as a function of temperature and fast neutron fluence (the symbols are explained in the text).

Fig. 2 Theoretically predicted swelling behaviour of annealed stainless steel AISI type 304 at a fast fluence of 10^{23}n cm^{-2}

- - - - - - - -	nucleation-growth model (26) (model 1)
-·-·-·-·-·-·-·-	nucleation-growth model, voids acting as principal sinks for point defects (27) (model 1')
————————	nucleation-growth model, including saturation of void nucleation at any temperature (28) (model 2)

Fig. 3 Theoretically predicted swelling behaviour of annealed stainless steel AISI type 304 at a fast fluence of 3.10^{23}n cm^{-2}

- - - - - - - -	nucleation-growth model (26) (model 1)
————————	nucleation-growth model, including saturation of void nucleation at any temperature (28) (model 2)

Fig. 4 The $(\frac{\Delta V}{V}, \Phi)$ plot according to equation 3 and to model 2 (see fig. 2,3) at 500°C. This plot demonstrates the nearly linear relation between fluence and swelling predicted by theory (curve a) and the higher power relation between fluence and swelling according to empirical equation 3 (curve b).

Fig. 5 Swelling in nickel-base alloys (32).

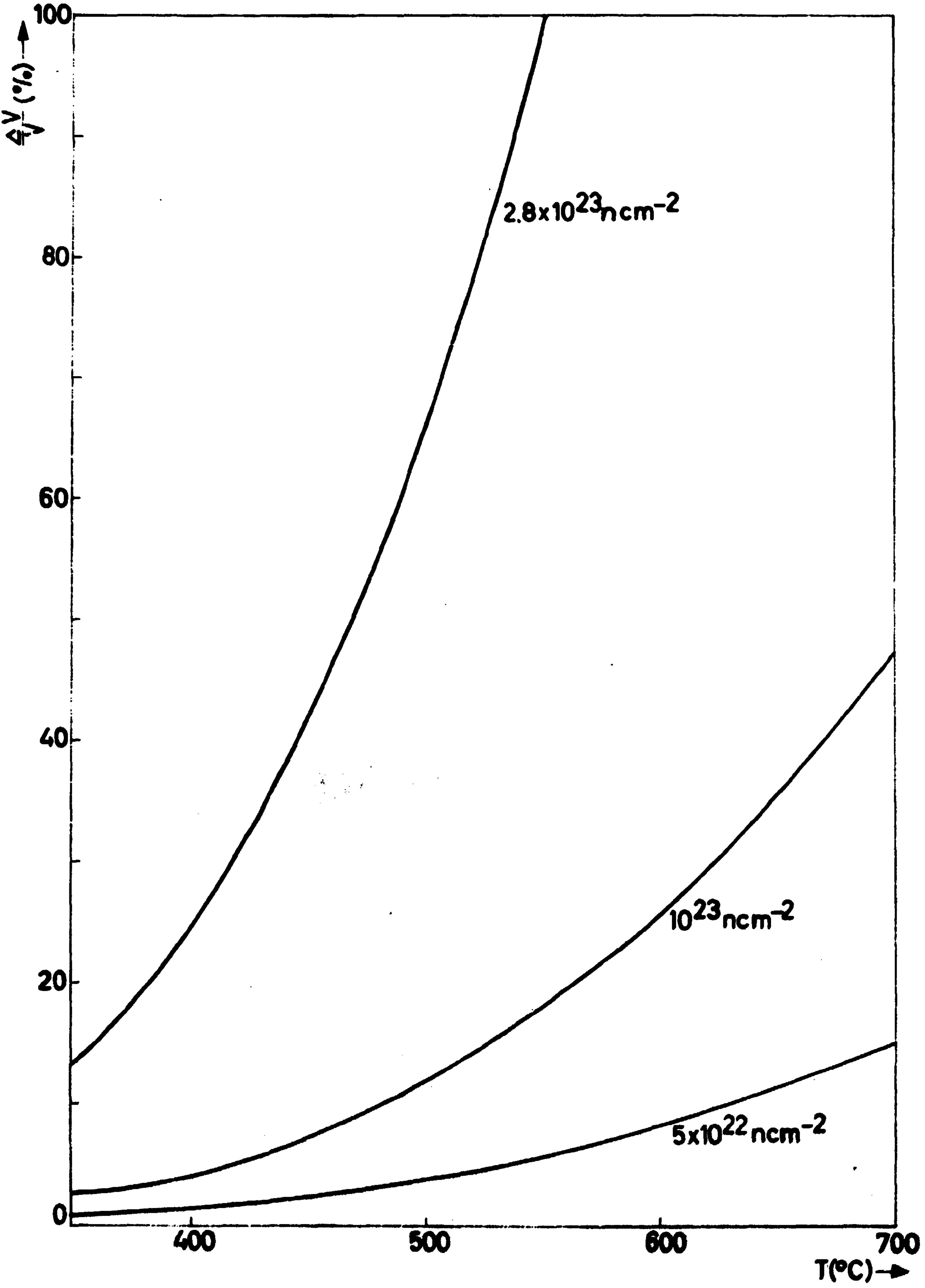
$\frac{\Delta V}{V}$ (%) →
100
80
60
40
20
0
400
500
600
700
T(°C) →
2.8×10^{23} n cm^{-2}
10^{23} ncm^{-2}
5×10^{22} ncm^{-2}

fig.1a

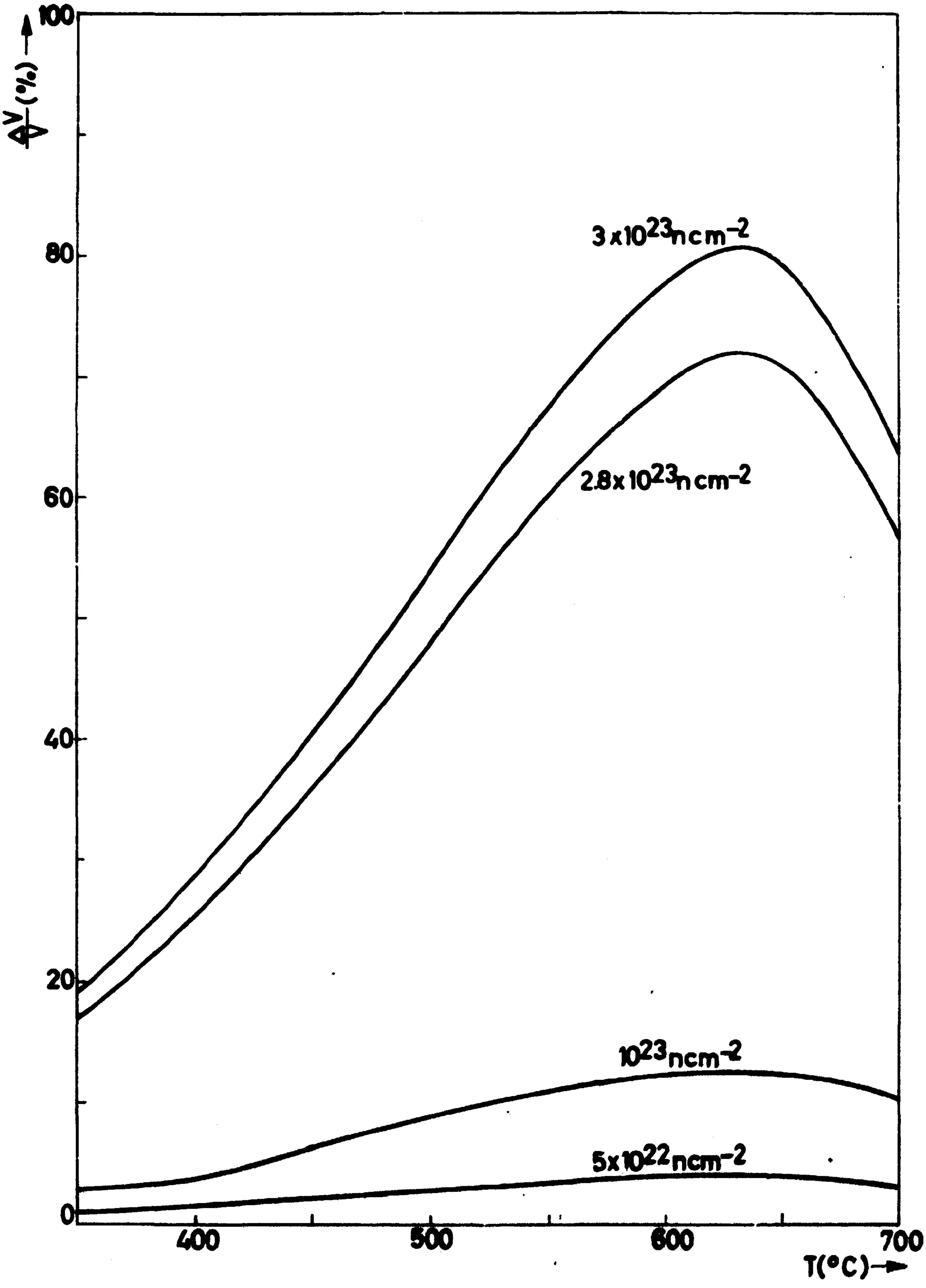

$\frac{\Delta V}{V}$ (%)
100
80
60
40
20
0
400
500
600
700
T(°C)
3×10^{23} n cm^{-2}
2.8×10^{23} n cm^{-2}
10^{23} n cm^{-2}
5×10^{22} n cm^{-2}

fig.1b

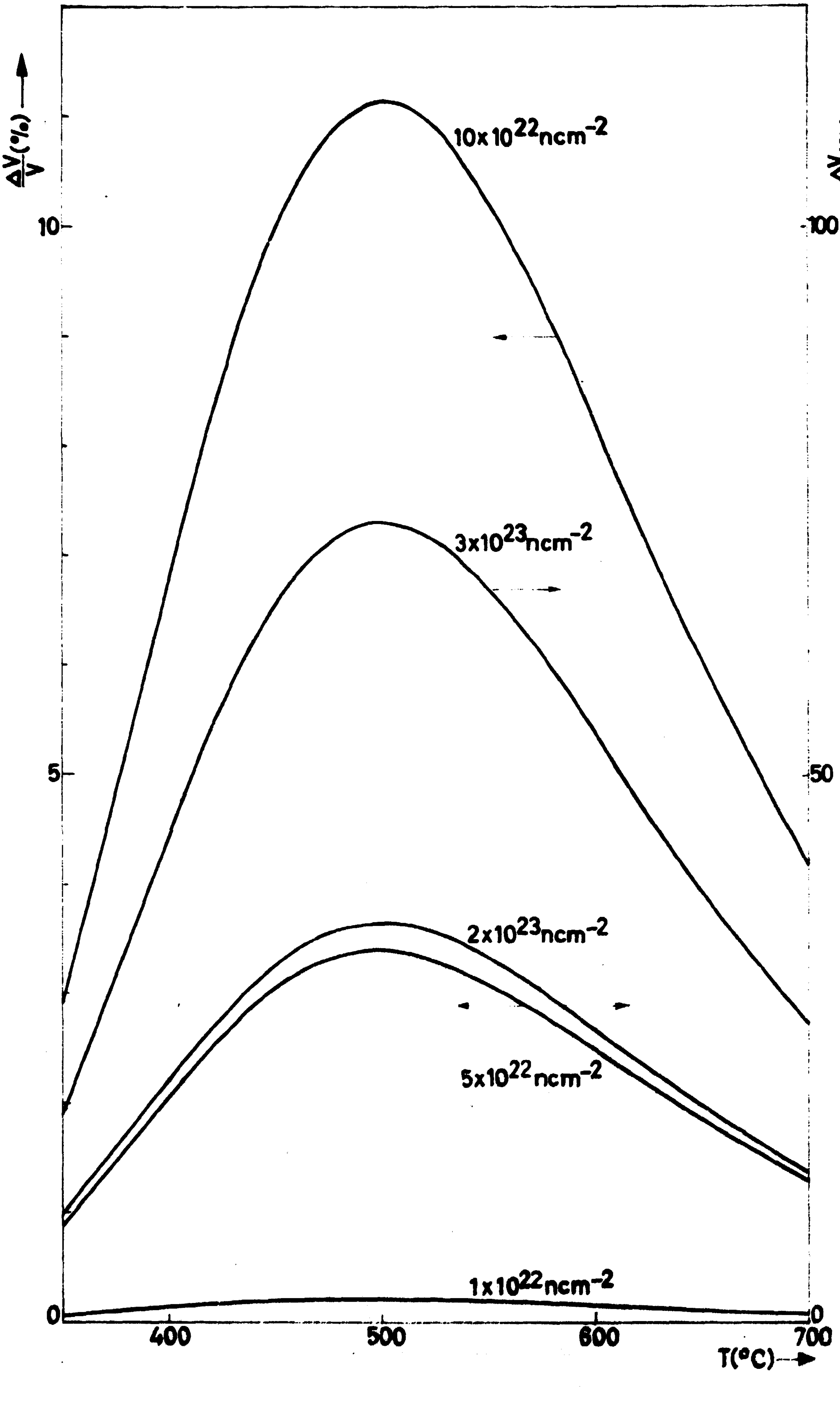

$\frac{\Delta V}{V}$(%)
$\frac{\Delta V}{V}$(%)
10
5
0
100
50
0
10×10^{22} ncm^{-2}
3×10^{23} ncm^{-2}
2×10^{23} ncm^{-2}
5×10^{22} ncm^{-2}
1×10^{22} ncm^{-2}
400
500
600
700
T(°C)

fig. 1c

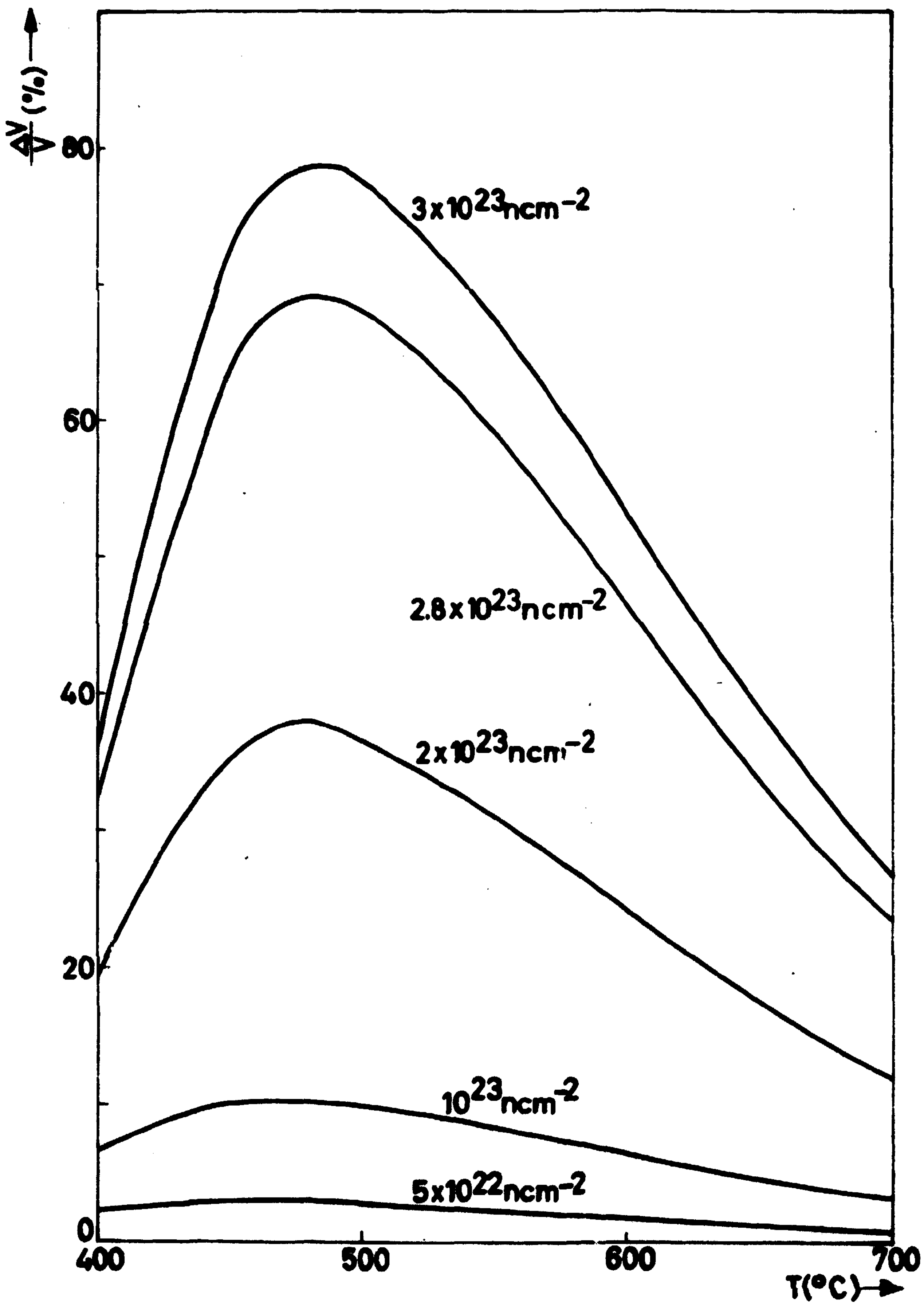

$\frac{\Delta V}{V}$ (%)
80
60
40
20
0
400
500
600
700
T(°C)
3×10^{23} ncm^{-2}
2.8×10^{23} ncm^{-2}
2×10^{23} ncm^{-2}
10^{23} ncm^{-2}
5×10^{22} ncm^{-2}

fig.1d

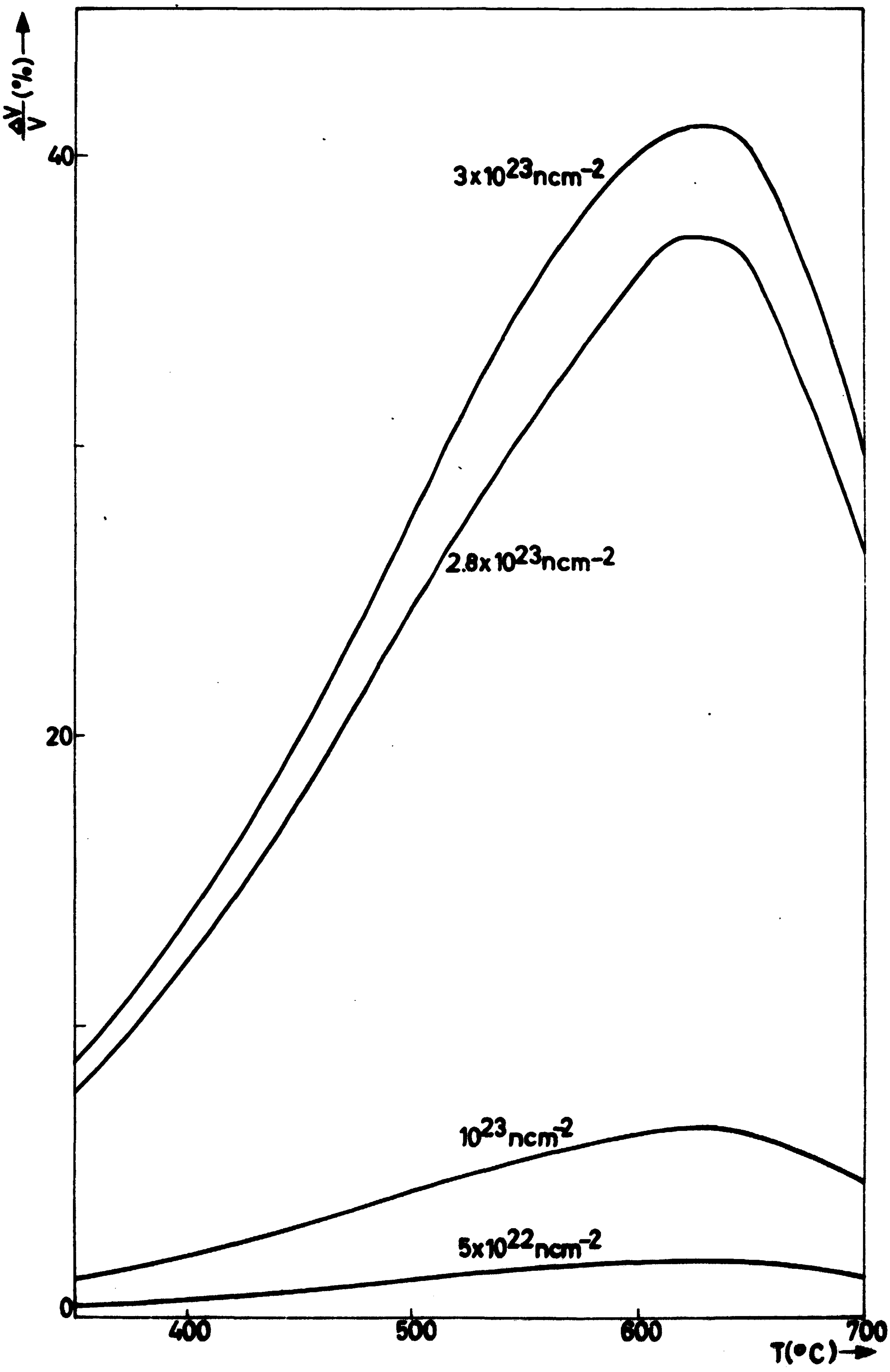

$\frac{\Delta V}{V}$ (%)
40
20
0
400
500
600
700
T(°C)
$3 \times 10^{23} ncm^{-2}$
$2.8 \times 10^{23} ncm^{-2}$
$10^{23} ncm^{-2}$
$5 \times 10^{22} ncm^{-2}$

fig.1e

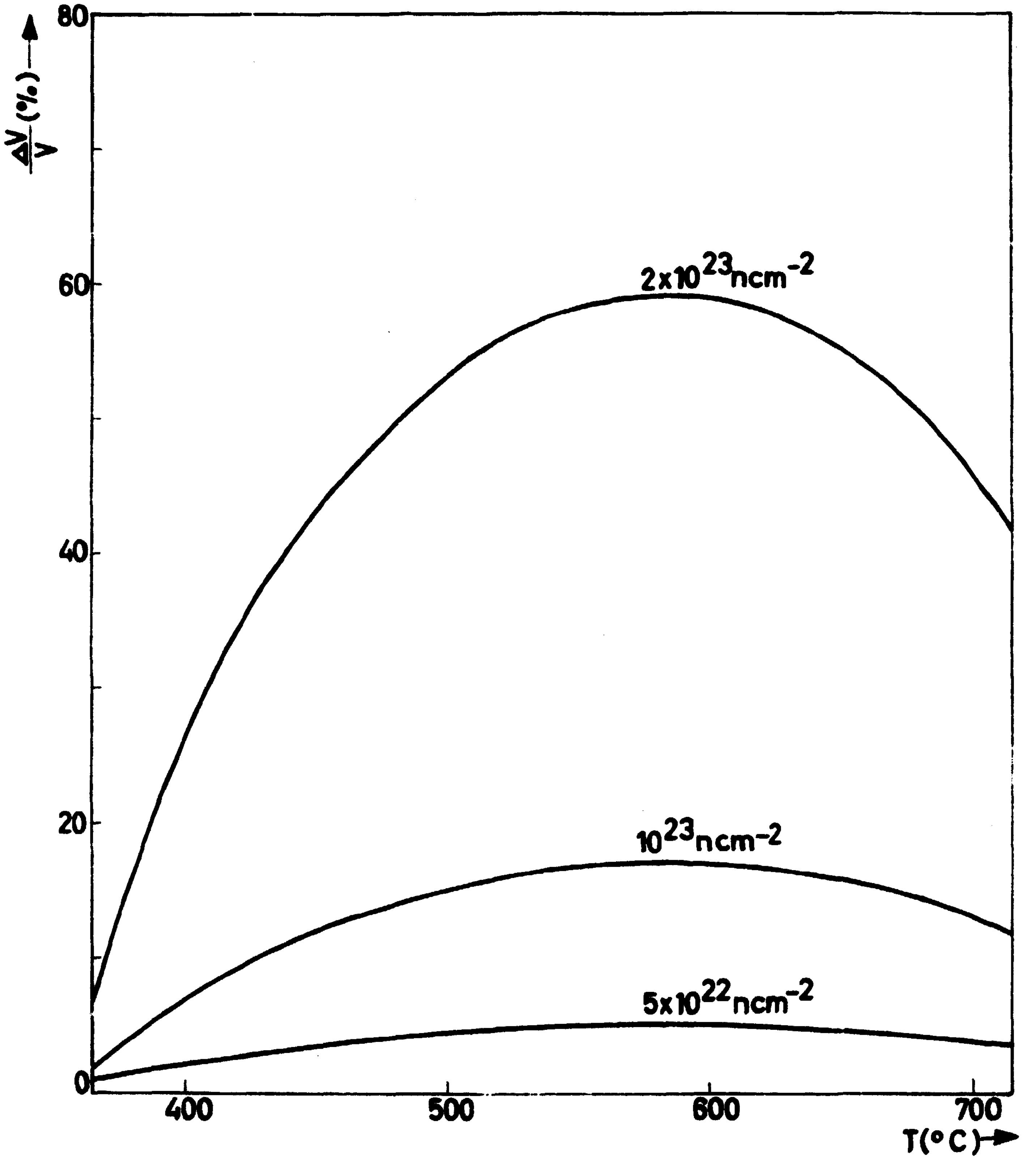
$\frac{\Delta V}{V}$ (%)
80
60
40
20
0
400
500
600
700
T(°C)
2×10^{23} ncm^{-2}
10^{23} ncm^{-2}
5×10^{22} ncm^{-2}

fig.1f

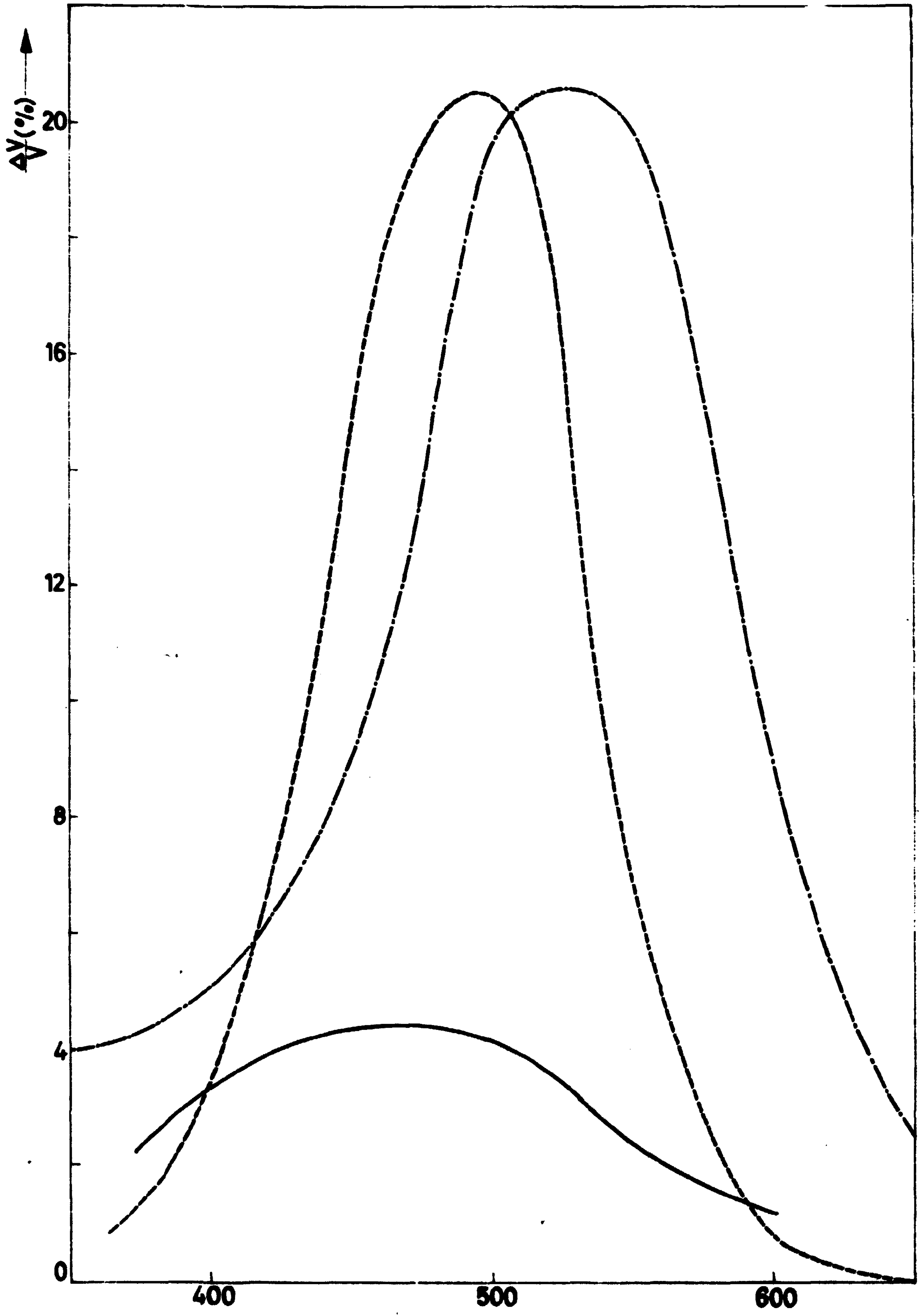

fig.2

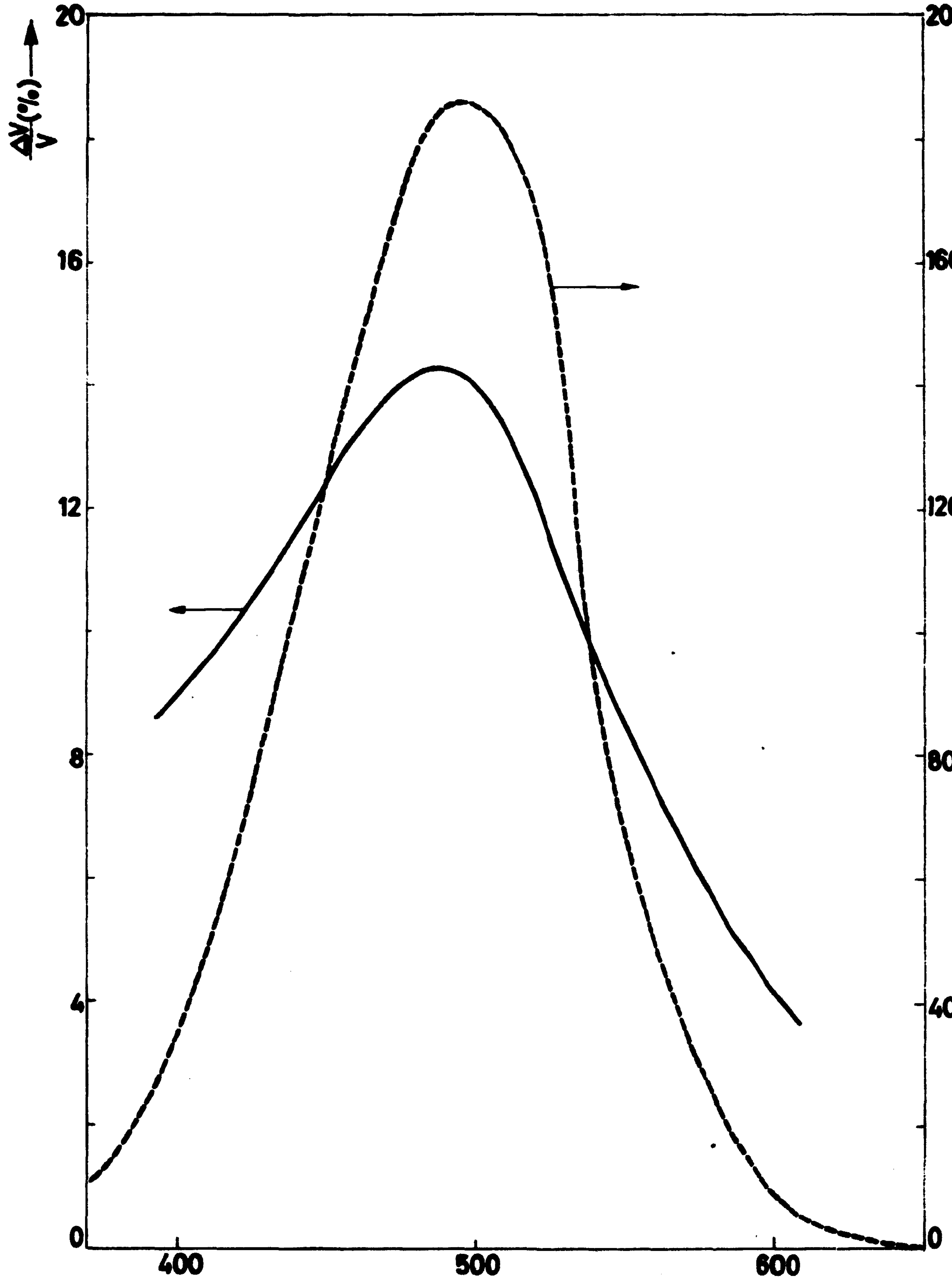

fig. 3

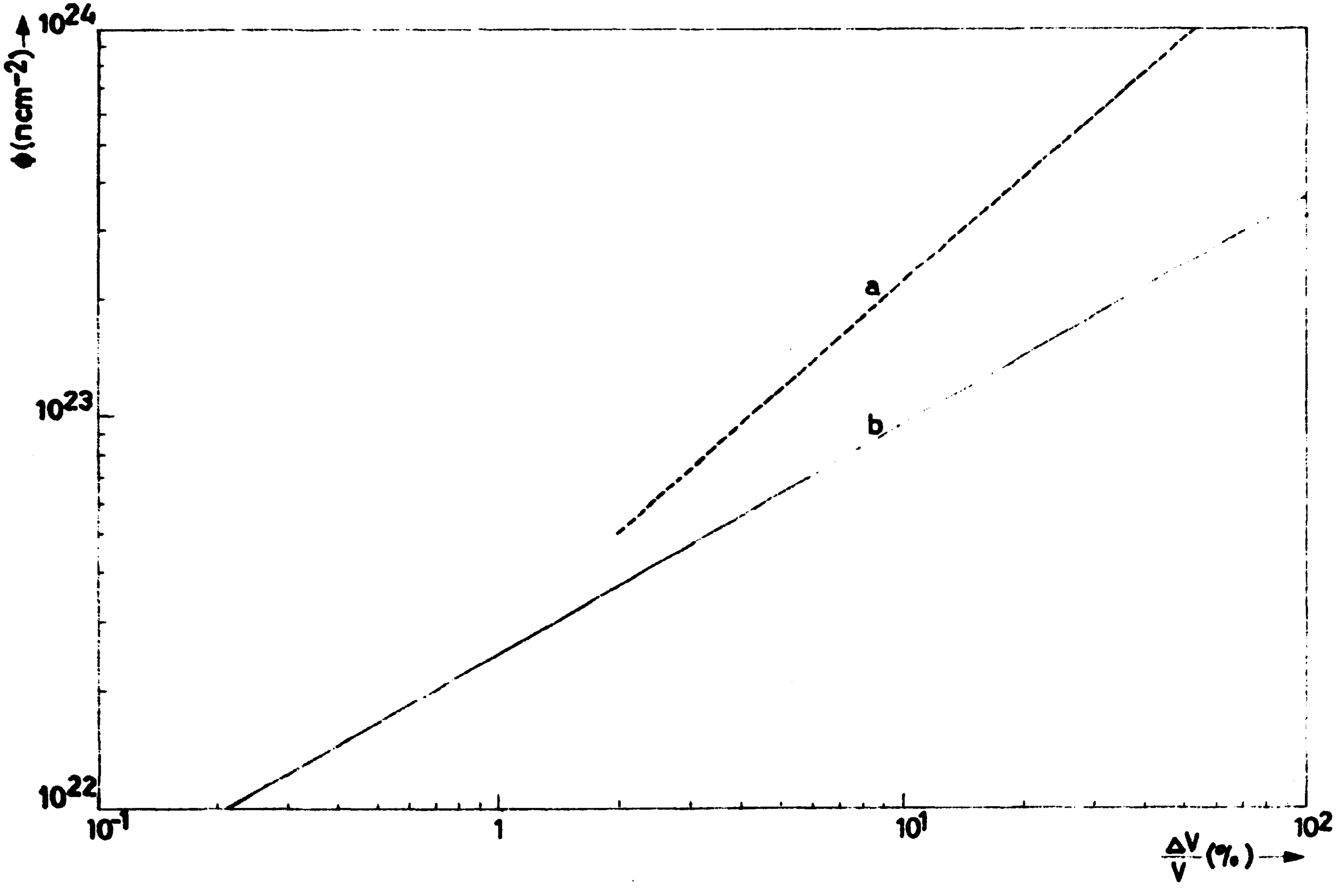

fig.4

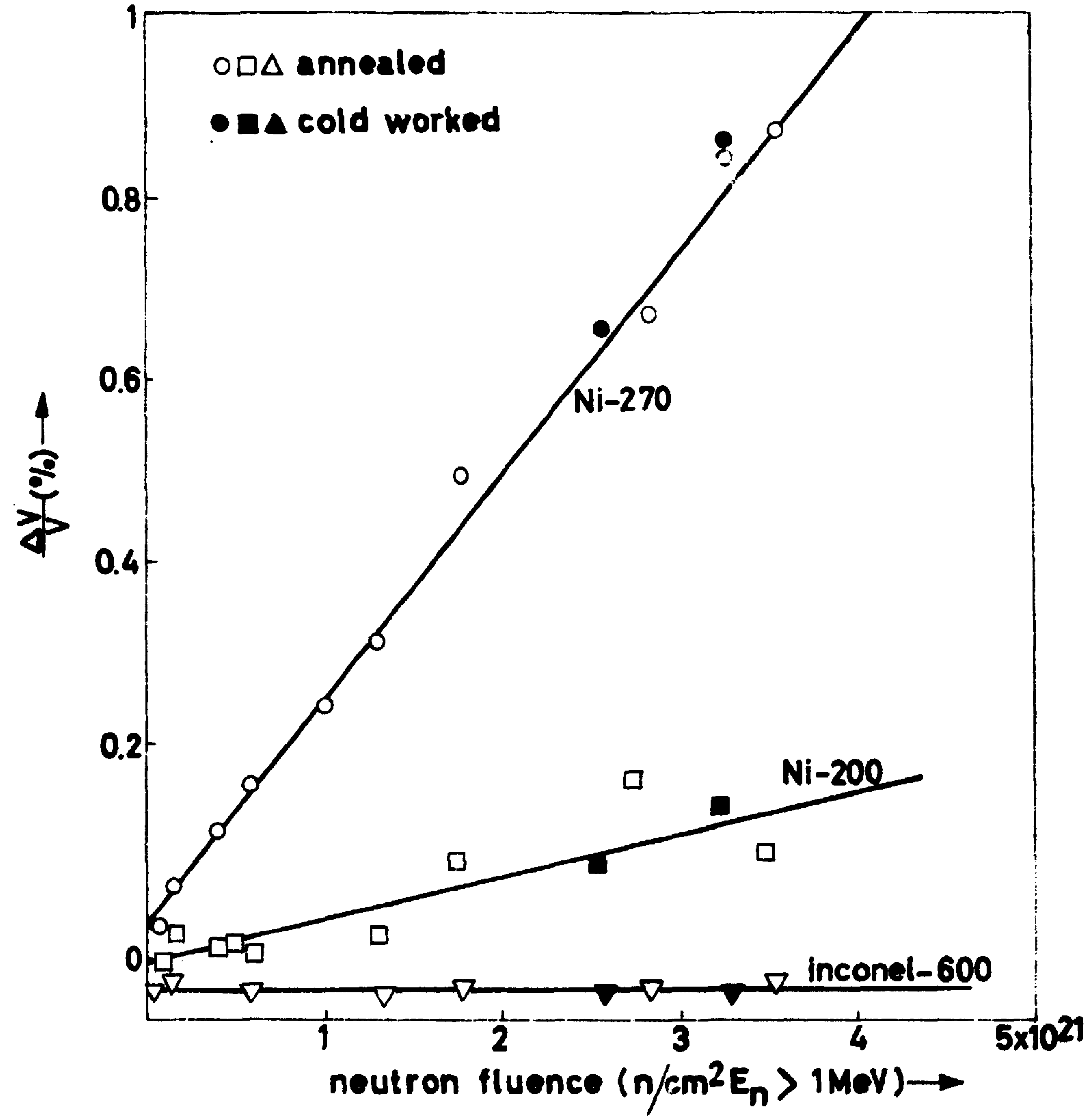
○□△ annealed
●■▲ cold worked
Ni-270
Ni-200
inconel-600
$\frac{\Delta V}{V}$ (%)
1
0.8
0.6
0.4
0.2
0
1
2
3
4
5x10²¹
neutron fluence (n/cm² E_n > 1MeV)

fig. 5